IL NUOVO CIMENTO **47 C** (2024) 10
DOI 10.1393/ncc/i2024-24010-7

COLLOQUIA: La Thuile 2023

# Rare and very rare decays of hyperons and heavy baryons at LHCb

G. MARTELLI(1)(2)(*) on behalf of the LHCb COLLABORATION

(1) *Dipartimento di Fisica e Geologia, Università degli studi di Perugia - Perugia, Italy*
(2) *INFN, Sezione di Perugia - Perugia, Italy*

received 10 October 2023

**Summary.** — This contribution presents the most recent results related to rare and very rare decays involving hyperons and heavy baryons at the LHCb experiment. The new results encompass the decays $\Lambda_b^0 \to D_s^- p$ and $\Xi_{cc}^{++} \to \Xi_c'^{+}\pi^+$, using data obtained from proton-proton collisions at a center-of-mass energy of 13 TeV during the LHC Run 2 data-taking, corresponding to a total integrated luminosity of $\sim 6$ fb$^{-1}$. Additionally, this contribution includes the investigation of the $\Sigma^+ \to p\mu^+\mu^-$ decay, which was already explored during Run 1, and outlines prospects for the ongoing Run 2 analysis.

## 1. – Introduction

Despite its remarkable accomplishments, the Standard Model (SM) continues to be an incomplete framework, leaving various unanswered questions in its wake. Many of its problems can be studied by exploring the flavour sector, delving into the properties and interactions of different particle flavours and the mixing between them. The Large Hadron Collider beauty (LHCb) experiment at CERN has proven itself to be an ideal setting for investigating flavour physics.

The LHCb detector [1] [2] is a single-arm forward spectrometer covering the pseudorapidity range $2 < \eta < 5$, designed for the study of particles containing $b$ or $c$ quarks. Within LHCb, the very rare decays search program continues to push the boundaries of particle physics by shedding light on the most elusive and intriguing processes involving hyperons and heavy baryons. In the next sections, recent LHCb results on the very rare $\Lambda_b^0 \to D_s^- p$ and $\Xi_{cc}^{++} \to \Xi_c'^{+}\pi^+$ decays are presented, following a review on the search for the $\Sigma^+ \to p\mu^+\mu^-$ decay conducted during Run 1 and prospects for the ongoing Run 2 analysis.

(*) E-mail: `gabriele.martelli@cern.ch`

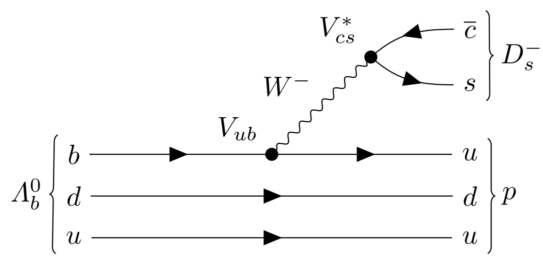


Fig. 1. – Tree-level diagram contributing to the $\Lambda_b^0 \to D_s^- p$ decay.

## 2. – First observation and branching fraction measurement of the $\Lambda_b^0 \to D_s^- p$ decay

The $\Lambda_b^0 \to D_s^- p$ decay is a weak hadronic decay proceeding through a $b \to u$ transition and described by a single leading-order diagram, as shown in fig. 1.

Its branching fraction is proportional to the square of the Cabibbo-Kobayashi-Maskawa (CKM) matrix element $|V_{ub}|$,

$$B(\Lambda_b^0 \to D_s^- p) \propto |V_{ub}|^2 |V_{cs}|^2 f_{D_s}^2 |a_{NF}|^2 |F_{\Lambda_b \to p}(m_{D_s}^2)|^2, \quad (1)$$

where $|V_{cs}|$ is the CKM matrix element describing the $c \to s$ quark transition, $f_{D_s}$ is the decay constant for the meson $D_s^-$, $F_{\Lambda_b \to p}$ is the form factor describing the $\Lambda_b^0 \to p$ transition and $|a_{NF}|$ quantifies the nonfactorisable effects such as final-state strong interactions leading to a nonfactorisable contribution in the decay amplitude.

Among the CKM matrix elements, $|V_{ub}|$ is the one with the smallest and most poorly determined magnitude. $b \to u$ transitions as in the $\Lambda_b^0 \to D_s^- p$ decay could enhance the current knowledge on $|V_{ub}|$ and serve as an input to check the consistency of the SM [3]. Furthermore, the $\Lambda_b^0 \to D_s^- p$ decay could provide a measure of the breaking factorisation hypothesis once the form factor for this decay is accurately evaluated [5].

The first observation and branching fraction measurement of the $\Lambda_b^0 \to D_s^- p$ decay is reported by the LHCb experiment [6]. The following results are obtained using proton-proton ($pp$) collision data collected at centre-of-mass energy of 13 TeV, corresponding to an integrated luminosity of 6 fb$^{-1}$, during the Run 2 of the Large Hadron Collider (LHC) between 2015 and 2018. The $\Lambda_b^0 \to \Lambda_c^+ \pi^-$ decay is chosen as normalisation channel, due to its topological similarity to the signal decay and relatively high branching fraction. Candidates for both signal and normalisation channels are reconstructed through the decays $D_s^- \to K^- K^+ \pi^-$ and $\Lambda_c^+ \to p K^- \pi^+$, respectively. The branching fraction of the $\Lambda_b^0 \to D_s^- p$ decay is evaluated as

$$\mathcal{B}(\Lambda_b^0 \to D_s^- p) = \mathcal{B}(\Lambda_b^0 \to \Lambda_c^+ \pi^-) \frac{N_{\Lambda_b^0 \to D_s^- p}}{N_{\Lambda_b^0 \to \Lambda_c^+ \pi^-}} \frac{\epsilon_{\Lambda_b^0 \to \Lambda_c^+ \pi^-}}{\epsilon_{\Lambda_b^0 \to D_s^- p}} \frac{\mathcal{B}(\Lambda_c^+ \to p K^- \pi^+)}{\mathcal{B}(D_s^- \to K^- K^+ \pi^-)}, \quad (2)$$

where $N_X$ is the measured yield and $\epsilon_X$ the efficiency of the reconstructed and selected candidates of the decay $X$. $\mathcal{B}(D_S^- \to K^- K^+ \pi^-)$ and $\mathcal{B}(\Lambda_c^+ \to p K^- \pi^+)$ are the known branching fractions for the final states of the signal and normalisation channels, respectively.

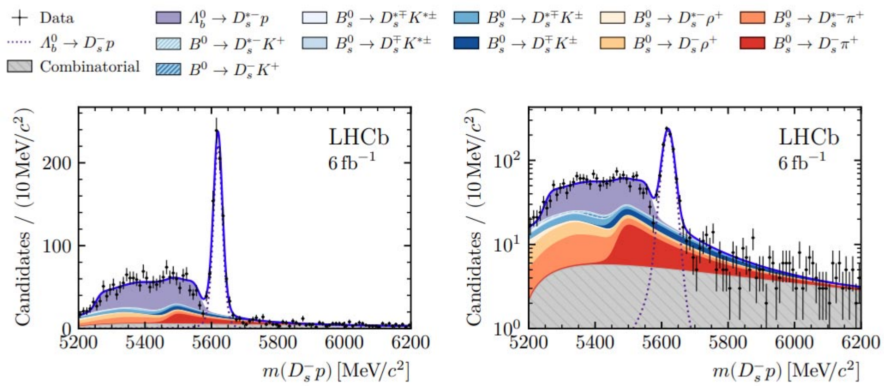


Fig. 2. – Invariant-mass distribution of $\Lambda_b^0 \to D_s^- p$ candidates, in (left) linear and (right) logarithmic scale, where the fit projections of the signal and background contributions are overlaid. The individual components in the fit are illustrated in the legend. Figures taken from [6].

While efficiencies are evaluated using simulated candidates and calibration data samples, yields are determined using unbinned maximum-likelihood fits to the $D_s^- p$ and $\Lambda_c^+ \pi^-$ invariant-mass distributions. The signal components are parametrised using the sum of a double-sided Hypatia function and a Johnson $S_U$ function while different parametrizations are applied for the background depending on its source. The fit to the invariant-mass distribution of $\Lambda_b^0 \to D_s^- p$ candidates is shown in fig. 2.

The $\Lambda_b^0 \to D_s^- p$ branching fraction can be evaluated using the measured efficiencies and yields, summarized in table I.

The measured $\Lambda_b^0 \to D_s^- p$ branching fraction is found to be

$$\mathcal{B}(\Lambda_b^0 \to D_s^- p) = (12.6 \pm 0.5 \pm 0.3 \pm 1.2) \times 10^{-6}, \tag{3}$$

where the third uncertainty is due to the uncertainty of the $\Lambda_b^0 \to \Lambda_c^+ \pi^-$, $D_s^- \to K^- K^+ \pi^-$ and $\Lambda_c^+ \to p K^- \pi^+$ branching fractions. This measurement will serve as input for future studies of factorisation in hadronic $\Lambda_b^0$ decays.

Table I. – *Obtained signal yields and efficiencies of the $\Lambda_b^0 \to D_s^- p$ and $\Lambda_b^0 \to \Lambda_c^+ \pi^-$ decays, as well as branching fractions used for this measurement* [7]. *The uncertainty on the signal yields and efficiencies is statistical.*

| | $\Lambda_b^0 \to D_s^- p$ | $\Lambda_b^0 \to \Lambda_c^+ \pi^-$ |
|---|---|---|
| Yield | $831 \pm 32$ | $(4.047 \pm 0.007) \times 10^5$ |
| Efficiency | $(0.1819 \pm 0.0013)\%$ | $(0.1947 \pm 0.0012)\%$ |
| $\mathcal{B}\left(\Lambda_b^0 \to \Lambda_c^+ \pi^-\right)$ | $(4.9 \pm 0.4) \times 10^{-3}$ | |
| $\mathcal{B}\left(D_s^- \to K^- K^+ \pi^-\right)$ | $(5.38 \pm 0.10) \times 10^{-2}$ | |
| $\mathcal{B}\left(\Lambda_c^+ \to p K^- \pi^+\right)$ | $(6.28 \pm 0.32) \times 10^{-2}$ | |

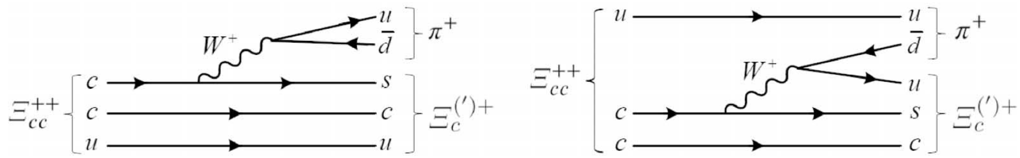


Fig. 3. – (Left) external and (right) internal $W$-emission diagrams of the $\Xi_{cc}^{++} \to \Xi_c^{\prime +}\pi^+$ decay.

## 3. – Observation of the doubly charmed baryon decay $\Xi_{cc}^{++} \to \Xi_c^{\prime +}\pi^+$

The quark model predicts the existence of baryons with two charm quarks and one light quark (either $u$, $d$, or $s$), making them excellent candidates for probing the validity of effective theories in the realm of Quantum ChromoDynamics (QCD). The $\Xi_{cc}^{++}$ is a heavy charmed baryon with a light quark $u$ discovered and studied by LHCb [8] with only a few decay modes known to date. The decay $\Xi_{cc}^{++} \to \Xi_c^{\prime +}\pi^+$ has been observed and its branching fraction relative to that of the normalisation channel $\Xi_{cc}^{++} \to \Xi_c^{+}\pi^+$ has been measured by the LHCb experiment [9] using $pp$ collisions collected at a centre-of-mass energy of 13 TeV, corresponding to an integrated luminosity of 5.4 fb$^{-1}$. The Feynman diagrams for the $\Xi_{cc}^{++} \to \Xi_c^{\prime +}\pi^+$ decay, outlining the external and internal $W$-emission contributions to the decay amplitude, are illustrated in fig. 3.

The $\Xi_{cc}^{++} \to \Xi_c^{\prime +}\pi^+$ is partially reconstructed, with the photon from the $\Xi_c^{\prime +} \to \Xi_c^{+}\gamma$ decay not reconstructed. The $\Xi_c^{+}$ is reconstructed from the $\Xi_c^{+} \to pK^-\pi^+$ final state for both signal and normalisation modes.

The branching fraction of the signal decay relative to that of the normalisation channel is defined as

$$\frac{\mathcal{B}\left(\Xi_{cc}^{++} \to \Xi_c^{\prime +}\pi^+\right)}{\mathcal{B}\left(\Xi_{cc}^{++} \to \Xi_c^{+}\pi^+\right)} = \frac{N_{\Xi_c^{\prime +}}}{N_{\Xi_c^{+}}} \times \frac{\epsilon_{\Xi_c^{+}}}{\epsilon_{\Xi_c^{\prime +}}}, \tag{4}$$

where $N_X$ is the measured yield and $\epsilon_X$ the total efficiency for the decay $X$.

The signal yield is determined by performing an unbinned maximum-likelihood fit to the $\Xi_c^{+}\pi^+$ invariant mass distribution in data while the efficiency is evaluated from simulated samples. The $\Xi_c^{+}\pi^+$ distribution is divided into Trigger On Signal (TOS) and Trigger Independent from Signal (TIS) samples, as defined in ref. [10]. The fit is performed on the $M(\Xi_c^{+}\pi^+) \equiv m(\Xi_c^{+}\pi^+) - m(\Xi_c^{+}) + m_0(\Xi_c^{+})$ distribution, with $m(\Xi_c^{+}\pi^+)$ and $m(\Xi_c^{+})$ being the $\Xi_c^{++}$ and $\Xi_c^{+}$ reconstructed invariant masses and $m_0(\Xi_c^{+})$ the known PDG mass [7]. The $\Xi_{cc}^{++} \to \Xi_c^{+}\pi^+$ reconstructed mass distribution is described by a Crystal Ball function while $\Xi_{cc}^{++} \to \Xi_c^{\prime +}\pi^+$ is parametrized by a linear function describing the true mass distribution of the signal convoluted with the Gaussian mass resolution $\sigma$. The fitted TOS and TIS invariant-mass distributions for the $\Xi_{cc}^{++}$ reconstructed and selected candidates are shown in fig. 4.

Including all systematic uncertainties, the measured relative branching fraction in the TOS and TIS samples are $1.81 \pm 0.43 \pm 0.25$ and $1.34 \pm 0.19 \pm 0.11$, respectively. Here the first uncertainty is statistical and the second systematic. The combination of the two measurements leads to

$$\frac{\mathcal{B}(\Xi_{cc}^{++} \to \Xi_c^{\prime +}\pi^+)}{\mathcal{B}(\Xi_{cc}^{++} \to \Xi_c^{+}\pi^+)} = 1.41 \pm 0.17 \pm 0.10. \tag{5}$$

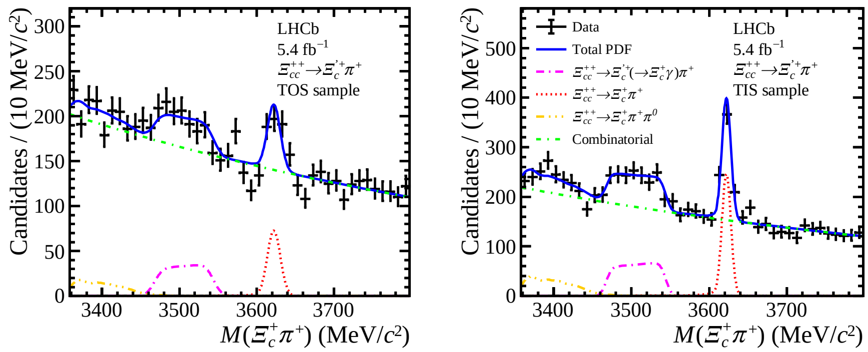


Fig. 4. – Reconstructed invariant-mass distribution of the $\Xi_{cc}^{++}$ candidates from the (left) TOS and (right) TIS samples, with the results of the fit overlaid. The $\Xi_{cc}^{++} \to \Xi_c'^{+}\pi^+$ component is shown as a purple dashed line, the $\Xi_{cc}^{++} \to \Xi_c^{+}\pi^+$ component as a red dotted line, the $\Xi_{cc}^{++} \to \Xi_c^{+}\pi^+\pi^0$ component as a yellow dashed line and the combinatorial component as a green dashed line. Figures taken from [9].

The result is not consistent with present theoretical predictions [11] and will provide inputs for future calculations.

## 4. – Evidence for the rare decay $\Sigma^+ \to p\mu^+\mu^-$

The $\Sigma^+ \to p\mu^+\mu^-$ decay is an $s \to d$ Flavour-Changing-Neutral-Current (FCNC) process, allowed only at loop level in the SM. The SM Feynman diagrams for this process are shown in fig. 5

The short-distance SM contributions are suppressed, with an estimated rate of $10^{-12}$ [12], leading to the process to be dominated by long-distance contributions and with a predicted branching fraction of

$$1.6 \times 10^{-8} < \mathcal{B}(\Sigma^+ \to p\mu^+\mu^-) < 9.0 \times 10^{-8}. \tag{6}$$

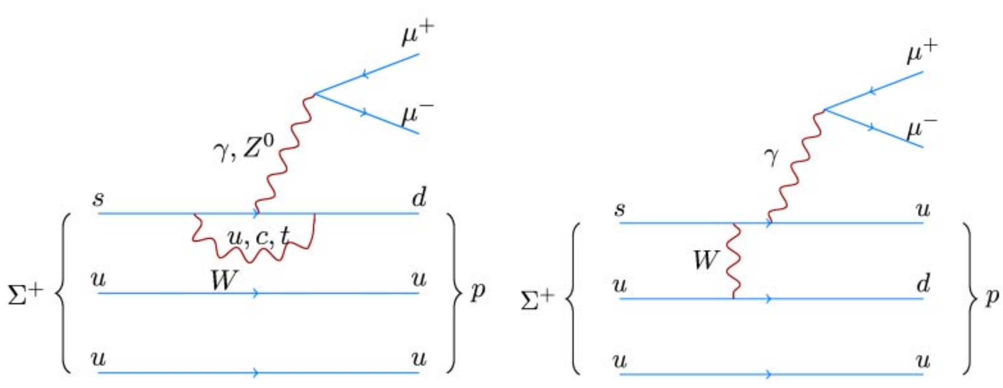


Fig. 5. – Feynman diagrams for the $\Sigma^+ \to p\mu^+\mu^-$ decay in the SM.

The HyperCP experiment reported an evidence of this decay based on three observed events on top of a negligible background [13]. The measured branching fraction is

$$\mathcal{B}(\Sigma^+ \to p\mu^+\mu^-) = (8.6^{+6.6}_{-5.4} \pm 5.5) \times 10^{-8}, \tag{7}$$

which would be compatible with the SM on the upper side of the foreseen branching fraction. The main feature of this evidence is that the three observed events have almost the same dimuon invariant mass. Their mass average value is $m_{X^0} = 214.3 \pm 0.5$ MeV/$c^2$. Such an evidence, if confirmed, would point towards a decay with an intermediate particle coming from the $\Sigma^+$ and decaying into two muons, *i.e.*, a $\Sigma^+ \to pX^0(\to \mu^+\mu^-)$ decay, which would constitute an evidence of physics beyond the SM. When correcting the efficiency for the different phase space under the $\Sigma^+ \to pX^0(\to \mu^+\mu^-)$ hypothesis, the measured branching fraction becomes

$$\mathcal{B}(\Sigma^+ \to pX^0(\to \mu^+\mu^-)) = (3.1^{+2.4}_{-1.9} \pm 5.5) \times 10^{-8}. \tag{8}$$

Various explanations beyond the SM have been proposed to explain this evidence. In general, a pseudoscalar particle is favoured over a scalar particle and a lifetime of the order of $10^{-14}$ s is estimated.

A search for the rare decay $\Sigma^+ \to p\mu^+\mu^-$ has been performed at LHCb with data recorded at center-of-mass energies $\sqrt{s} = 7$ and 8 TeV during Run 1, corresponding to an integrated luminosity of 3 fb$^{-1}$ [14]. The branching fraction is evaluated as

$$\mathcal{B}(\Sigma^+ \to p\mu^+\mu^-) = \frac{\epsilon_{\Sigma^+ \to p\pi^0}}{\epsilon_{\Sigma^+ \to p\mu^+\mu^-}} \frac{\mathcal{B}(\Sigma^+ \to p\pi^0)}{N_{\Sigma^+ \to p\pi^0}} N_{\Sigma^+ \to p\mu^+\mu^-}, \tag{9}$$

with $\Sigma^+ \to p\pi^0$ chosen as the normalisation channel and $N(X)$, $\epsilon(X)$ the yield and efficiencies of the decay X. While the yields are evaluated from a binned extended maximum likehood fit to the invariant mass distributions, the efficiencies are estimated from fully simulated samples. The observed number of signal $\Sigma^+ \to p\mu^+\mu^-$ is obtained with a fit to the $p\mu^+\mu^-$ invariant-mass distribution in the range $1149.6 < m_{\mu^+\mu^-} < 1409.6$ MeV/$c^2$. The invariant mass distribution, with the signal described by an Hypatia function and the combinatorial background with a modified ARGUS function, is shown in fig. 6(A). The spectrum of the dimuon invariant mass, presented in fig. 6(B) is compatible with a phase space distribution, *i.e.*, no significant sign of a resonant contribution is present, in contrast with the previous result from the HyperCP experiment.

The measured branching fraction is

$$\mathcal{B}(\Sigma^+ \to p\mu^+\mu^-) = (2.2^{+1.8}_{-1.3}) \times 10^{-8}, \tag{10}$$

which is consistent with the SM prediction. An upper limit on the branching fraction of

$$\mathcal{B}(\Sigma^+ \to pX^0(\to \mu^+\mu^-)) < 1.4 \times 10^{-8} \tag{11}$$

at 90% CL has been put which would exclude the HyperCP signal in the resonant hypothesis.

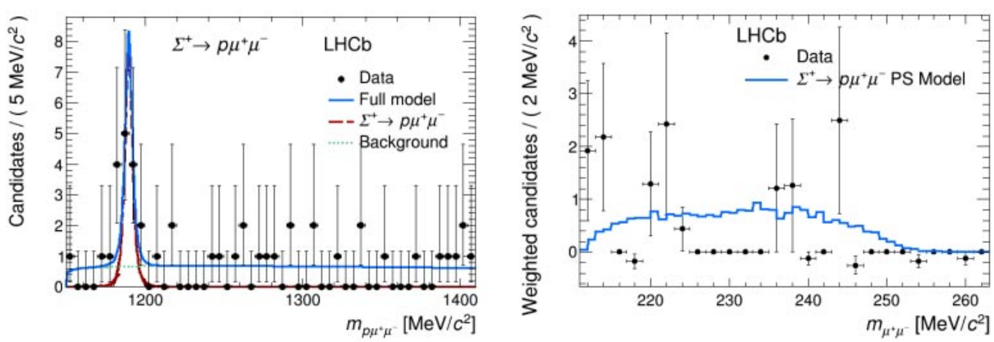


Fig. 6. – (A) Invariant mass distribution of $\Sigma^+ \to p\mu^+\mu^-$ candidates in data. (B) Background-subtracted distribution of the dimuon invariant mass for $\Sigma^+ \to p\mu^+\mu^-$ candidates, superimposed with the distribution from the simulated phase-space (PS) model. Uncertainties on data points are calculated as the square root of the sum of squared weights. Figures taken from [14].

**4**˙1. *Prospects for the ongoing Run2 analysis*. – A new search for the $\Sigma^+ \to p\mu^+\mu^-$ decay is ongoing within the LHCb experiment using *pp* collision data recorded at center-of-mass energies $\sqrt{s} = 13$ TeV, corresponding to an integrated luminosity of 5.6 fb$^{-1}$. An increase in dataset size of a factor $\sim 4$ compared to the Run 1 result is expected, based on scaling of luminosity and cross-section. With respect to the previous analysis, dedicated triggers have been implemented since 2016. Therefore, a significant gain in efficiency, approximately by a factor $\sim 10$, is also expected. Thanks to these new advantages, it is now possible to measure observables with greater precision. A clear first observation of the decay is expected, followed by the measurement of other observables such as the differential branching fraction with respect to the dimuon mass and the forward-backward asymmetry in the decay. A "direct" CP asymmetry measurement is also possible as

$$\mathcal{A}_{CP} = \frac{\mathcal{B}(\Sigma^+ \to p\mu^+\mu^-) - \mathcal{B}(\bar{\Sigma}^+ \to \bar{p}\mu^+\mu^-)}{\mathcal{B}(\Sigma^+ \to p\mu^+\mu^-) + \mathcal{B}(\bar{\Sigma}^+ \to \bar{p}\mu^+\mu^-)}. \tag{12}$$

Results from this Run 2 analysis are expected soon.

## 5. – Conclusions

In summary, recent results on rare and very rare decays involving hyperons and heavy baryons at LHCb are reported. The new results rely on the data samples of *pp* collisions collected by the LHCb experiment at a centre-of-mass energy of 13 TeV, corresponding to a total integrated luminosity of $\sim 6$ fb$^{-1}$. The first observation of the $\Lambda_b^0 \to D_s^- p$ decay and its branching fraction measurement are presented alongside a new decay mode of the doubly charmed baryon $\Xi_{cc}^{++} \to \Xi_c^{\prime +}\pi^+$. Furthermore, the Run 1 measurement of the $\Sigma^+ \to p\mu^+\mu^-$ decay is revisited and prospects for the ongoing Run 2 analysis are introduced.

REFERENCES

[1] LHCb Collaboration (Alves A. A. jr. *et al.*), *JINST*, **3** (2008) S08005.
[2] LHCb Collaboration (Aaij R. *et al.*), *Int. J. Mod. Phys. A*, **30** (2015) 1530022, arXiv:1412.6352 [hep-ex].

[3] CKMfitter Group (Charles J. *et al.*), *Phys. Rev. D*, **91** (2015) 073007, arXiv:1501.05013v2 [hep-ph].
[4] LHCb Collaboration (Aaij R. *et al.*), *Eur. Phys. J. C*, **81** (2021) 314.
[5] Detmold W., Lehner C. and Meine S., *Phys. Rev. D*, **92** (2015) 034503, arXiv:1503.01421v3 [hep-lat].
[6] LHCb Collaboration (Aaij R. *et al.*), *JHEP*, **07** (2023) 075.
[7] Particle Data Group (Workman R. L. *et al.*), *Prog. Theor. Exp. Phys.*, **2022** (2022) 083C01.
[8] LHCb Collaboration (Aaij R. *et al.*), *Phys. Rev. Lett.*, **119** (2017) 112001.
[9] LHCb Collaboration (Aaij R. *et al.*), *JHEP*, **05** (2022) 038.
[10] Tolk S., Albrecht J., Dettori F. and Pellegrino A., *Data driven trigger efficiency determination at LHCb* CERN-LHCb-PUB-2014-039, http://cds.cern.ch/record/1701134.
[11] Sharma N. and Dhir R., *Phys. Rev. D*, **96** (2017) 113006.
[12] He X.-G., Tandean J. and Valencia G., *Phys. Rev. D*, **72** (2005) 074003.
[13] HyperCP Collaboration (Park H. *et al.*), *Phys. Rev. Lett.*, **94** (2005) 021801.
[14] LHCb Collaboration (Aaij R. *et al.*), *Phys. Rev. Lett.*, **120** (2018) 221803.